



Synchrotron infrared microspectroscopic analysis of collagens I, III, and elastin on the shoulders of human thin-cap fibroatheromas

David L. Wetzel^{a,*}, Ginell R. Post^b, Robert A. Lodder^c

^a Microbeam Molecular Spectroscopy Laboratory, Kansas State University, Shellenberger Hall, Manhattan, KS 66506-2201, USA

^b Department of Pathology and Laboratory Medicine, College of Medicine, University of Kentucky, Lexington, KY 40506-0082 USA

^c Chemistry Department, University of Kentucky, Lexington, KY 40506-0886, USA

Accepted 14 February 2005

Abstract

Of the many people who experience a sudden cardiac event (acute coronary syndromes and/or sudden cardiac death), a large portion has no prior symptoms. One potential *in vivo* spectroscopic technique for diagnosis of pathological conditions that underlie these sudden cardiac events involves the use of a near-infrared spectrometric catheter with moderate *in vivo* spatial resolution. To justify the time and expense of such an *in vivo* protocol, the putative vulnerable narrow region at the shoulder of the thin cap fibroatheroma is chemically characterized by high spatial resolution mid-infrared microspectroscopy. The sharp peaks of the mid-infrared and the previous band assignments that are readily available are useful in establishing the basis needed to support the development and validity of future *in vivo* NIR probing. The spatial resolution of *in vivo* NIR spectrometric catheters is limited by light scattering from blood and by the motion of the catheter and blood vessel wall, making it difficult to characterize a fibrous cap in the rupture zone. However, the spatial resolution of *in vitro* synchrotron IR microspectroscopy is high and probably sufficient to characterize chemically the actual area of disruption. A thin-cap fibroatheroma is a rupture-prone plaque. The shoulder of the cap (where the cap meets the vessel wall) is most vulnerable to rupture because mechanical stress at this point weakens the collagen and elastin fibers. It is hypothesized that the breakdown of elastin is highest in this target zone, followed by collagen III. The analysis of collagen I, collagen III, and elastin concentration in the small (ca. 10 μm) interface zone, between the intimal wall of the artery and the fibrous cap, is of concern because it is the shoulder where the protein degradation is expected to be the highest. (A similar degradation occurs on a larger scale in the vessel wall in abdominal aortic aneurysm.) For this reason, if confirmed, testing at this location would presumably offer the highest sensitivity and provide the earliest possible warning of rupture-prone plaque. In the current study, post-mortem human tissue was used. Future experiments will be performed on animal models where *in vivo* NIR catheterization is followed by post-mortem mid-infrared microspectroscopy on the same animal. Subsequently it may be possible to develop *in vivo* near-infrared spectrometric catheter techniques suitable for use with human subjects in a clinical setting.

© 2004 Elsevier B.V. All rights reserved.

Keywords: Collagens; Human; Fibroatheromas

1. Introduction

Cardiovascular disease has been the primary cause of death in industrialized countries for some time, and it is rapidly becoming the number one killer in the developing countries [1]. According to recent estimates, 61,800,000 Americans have one or more types of cardiovascular disease.

Each year, more than 1 million people in the United States and more than 19 million others worldwide suffer a sudden cardiac event (acute coronary syndromes and/or sudden cardiac death). A considerable segment of this population has no preceding symptom. There is a mandate for diagnosis and treatment of the pathologic conditions that lie beneath these sudden cardiac events, and identifying vulnerable plaques and patients.

The word “vulnerable” is used to denote the probability of exhibiting an event in the future. The word vulnerable has

* Corresponding author.

E-mail address: dlw@wheat.ksu.edu (D.L. Wetzel).

52 been employed in a variety of reports in the medical
53 literature, all of which portray conditions predisposed to
54 injury. In this respect, the term “vulnerable plaque” is most
55 appropriate to classify plaques susceptible to complications.
56 In contrast, interventional cardiologists and cardiovascular
57 pathologists retrospectively explain the plaque responsible
58 for coronary occlusion and death as a culprit plaque, apart
59 from its histopathologic appearance. However, for prospec-
60 tive evaluation, diagnosis, and treatment, clinicians require a
61 term like culprit for identifying such plaques before an event
62 occurs.

63 Plaque rupture is the most frequent type of plaque
64 complication, accounting for in excess of 70% of fatal
65 acute myocardial infarctions and/or sudden coronary
66 deaths. A number of retrospective autopsy series and a
67 handful of cross-sectional clinical studies have indicated
68 that thrombotic coronary death and acute coronary
69 syndromes are instigated by plaque features and associated
70 factors. The majority of methods for detecting and treating
71 vulnerable plaque are dedicated to rupture-prone plaque.
72 This class of plaque is commonly called a “thin-cap
73 fibroatheroma”.

74 A thin-cap fibroatheroma is typified by a large lipid core
75 rich in cholesterol and cholesterol esters. These plaques have
76 a cap thickness of less than 100 μm and a lipid core
77 accounting for greater than 40% of the plaque’s total volume
78 [2]. Potential *in vivo* intravascular diagnostic techniques
79 include optical coherence tomography (OCT), intravascular
80 ultrasonography (IVUS), elastography (palpography), MRI,
81 angiography, and near-infrared spectroscopy. Increasing
82 evidence substantiates that diverse types of vulnerable
83 plaque with differing histopathology and biology exist.
84 Autopsy [3] and IVUS studies [4] have demonstrated that
85 atherosclerotic lesions commonly exist in young and
86 asymptomatic persons. The percentage of these lesions that
87 represent morphologies of rupture-prone vulnerable plaques
88 remains to be determined. Furthermore, chronic inflamma-
89 tion [5] and macrophage/foam cell formation are a
90 fundamental element of the natural history of atherosclero-
91 sis. To assess plaque vulnerability, it is apparent that a
92 collective methodology able to appraise structural char-
93 acteristics (morphology) as well as functional properties
94 (activity) of plaque will likely be most revealing, and may
95 offer higher prognostic value than a single method.

96 Among the first changes in the arterial wall in
97 atherosclerosis is an increase in retained lipoproteins and
98 ensuing oxidation in the subendothelial matrix [5]. Develop-
99 ment of lipid-laden macrophages (foam cells) is another
100 characteristic of the early atherosclerotic progression.
101 Proliferation and phenotypic alterations in smooth muscle
102 cells are also observed. The highly developed atherosclero-
103 tic lesion may be distinguished by amassing of extracellular
104 lipid, growth of a lipid-rich necrotic core, establishment of a
105 fibrous cap, and calcification. Atherosclerosis in the arterial
106 wall is associated with aneurysm, although it is not clear that
107 this is an underling contributory relationship.

Abdominal aortic aneurysms (AAAs) are potentially life- 108
threatening conditions that arise in up to 10% of the elderly 109
populations in industrialized nations. Similar fibrous protein 110
composition changes have been observed in both the plaque 111
cap in atherosclerosis and in the media and adventitia of 112
AAAs. However, an aneurysm is roughly defined as a 113
permanent dilatation of an artery limited to a small area. 114
AAAs occur due to considerable remodeling of the 115
extracellular matrix and are regularly accompanied by 116
atherosclerosis. They may be manifested by catastrophic 117
rupture, markers of pressure on other viscera, or an 118
embolism initiating in the aneurysm wall, but most are 119
asymptomatic. Collagen and elastin are the main structural 120
components of vessel walls that have been broadly 121
implicated in aneurysm formation, progression, and rupture. 122
These same proteins are found in the cap of fibroatheromas. 123
The prevailing structural modification linked with human 124
AAAs that has been reported is a loss in elastin 125
concentration in the aortic wall. Significant correlations 126
between lowering elastin concentration and increasing AAA 127
diameter have been noted. One proposed mechanism for 128
reduced elastin concentrations is degradation or loss brought 129
about by elastolysis. Although there have been differences in 130
the findings of many studies, it is clear that increases in the 131
collagen-to-elastin ratio are a universal observation in 132
AAAs. Analytical methods capable of analyzing collagen 133
and elastin content of arteries *in vivo* could be valuable in the 134
diagnosis of aneurysm and atherosclerosis, and might even 135
permit prediction of future clinical events. 136

Diffuse reflection near-infrared spectroscopy has proven 137
to be a useful technique for identifying chemical content of 138
atherosclerotic tissues [7]. Our laboratory has described the 139
use of near-IR spectroscopy to categorize human aortic 140
atherosclerotic plaques and to quantify cholesterol, HDL, 141
and LDL in arterial wall samples [8,9]. In a previously study 142
[6], our laboratory also published the near-infrared spectra 143
of collagen I, III, and elastin. The collagens and elastin 144
possess distinctive near-IR spectra that permit identification 145
and quantification in tissue samples. The data presented in 146
this report show that collagen I, III, and elastin also have 147
distinctive mid-infrared spectra. While the precise relation- 148
ship between mid-IR fundamental signals and near-IR 149
overtone and combination signals is not always clear, the 150
fact that these target analytes are distinguishable in both 151
spectral regions increases the likelihood that clinical 152
observations made in the IR *in vitro* will translate into 153
some form that is useful diagnostically in the near-IR in 154
vivo. 155

In contrast to the mid-IR, near-IR spectrometry is 156
characterized by low molar absorptivities and broad 157
overlapping bands. *In vivo* vibrational spectrometry has 158
been plagued historically by problems with high water 159
absorbance in tissue, light scattering, peak overlap, and peak 160
shifting with temperature and sample-matrix composition. 161
The intense absorbance of water more than any other factor 162
prevents the use of mid-IR spectrometry as a catheter-based 163

164 diagnostic tool in atherosclerosis. Instead, near-IR spectro-
165 metry has been driven into increasingly complex biological
166 and medical problems as more intense and more stable light
167 sources as well as more efficient detectors (and in many
168 cases, more efficient imaging detectors) have been devel-
169 oped. Improved methods of obtaining rapid wavelength
170 selectivity using tunable lasers [10] and integrated sensing
171 and processing using molecular factor filters [11] are also
172 playing an important role in advancing near-IR spectrometry
173 in a clinical setting.

174 Synchrotron infrared light is approximately 1000 times
175 more intense than a conventional infrared source. In
176 addition, synchrotron infrared light is highly collimated
177 like a laser, making it more easily focused onto a small spot.
178 However, unlike a laser, the synchrotron emits a wide range
179 of infrared wavelengths, enabling FTIR microspectroscopy.
180 Consequently, with synchrotron infrared light, samples can
181 be studied that are smaller and/or more dilute in
182 concentration. In addition, the 1000-fold increase in
183 brightness translates to data collection times that are about
184 30 times faster with the synchrotron source in comparison to
185 a global source. For this study, use of intense synchrotron
186 radiation permits small microscopic apertures near the
187 diffraction limit of the light to be used in microspectrometry,
188 increasing the spatial resolution of collagens and elastin
189 attainable at the site of plaque rupture. Measuring IR
190 fundamentals provides stronger signals with less peak
191 overlap than available with NIR overtone and combination
192 bands.

193 Infrared spectrometry has been employed a number of
194 times in the analysis of arterial collagens and elastin. Human
195 arterial tissue has been characterized using FT-IR micro-
196 spectroscopy and chemometrics [12,13]. Comparative
197 studies of plaques and proteins using FTIR and other
198 methods have been performed [14]. Collagen modifications
199 and surface properties of arteries have been studied in a
200 bovine model¹⁵. The effect of elastin on the calcification of
201 collagen–elastin matrix systems has been studied with
202 infrared spectrometry [16]. Finally, fundamental vibrational
203 information on collagens and elastin has been derived from
204 studies using FT-Raman spectrometry [13,17].

205 Similar composition changes have been observed in both
206 the fibrous cap of lesions in atherosclerosis and in the media
207 and adventitia of AAAs, albeit on different physical scales
208 [15,18,19]. Near-infrared spectrometry, immunohistochem-
209 istry, and scanning electron microscopy with morphometry
210 have been employed in these studies of collagen and elastin
211 composition changes. The spectrometric correlation meth-
212 odology employed in the following study relies on collagen
213 and elastin content changing within the samples as
214 suggested by previous research. This preliminary study
215 tests the hypothesis that the changes observed previously in
216 collagen I, III, and elastin in aneurysm on a millimeter scale
217 are similar to the changes that occur in the fibrous cap of
218 vulnerable atherosclerotic plaque on a scale of micrometers
219 or tens of micrometers. If successfully demonstrated, the

220 similarities could be used as in vivo markers of the
221 vulnerable plaques most in need of treatment, and could be
222 used in monitoring therapies in atherosclerotic plaques
223 treated by drugs.

2. Experimental 224

2.1. Tissue samples 225

226 Twenty human coronary tissue sections were obtained
227 post-mortem without identifiers from a single patient
228 through the University of Kentucky Medical Center, Clinical
229 Pathology Services. The study was approved by the
230 University of Kentucky IRB and HIPAA compliance office.
231 If components other than collagen and elastin were in the
232 tissue and were varying in concentration, then the
233 correlation maps produced by IR imaging would be biased
234 and would not likely reflect the individual contributions
235 from collagen I, III and elastin in the sample. The potential
236 for bias was eliminated by removing all other components of
237 the tissue visible on IR spectra by a washing, solvent-
238 extraction and formalin-fixing process prior to mounting the
239 tissue sections on the slides⁷. The tissue sections were
240 mounted in paraffin onto two low-e glass slides (SensIR) for
241 infrared microspectrometry. A visible light image of a
242 stained section of human coronary atherosclerotic plaque
243 appears in Fig. 1. This section was adjacent to the section
244 used for IR microspectrometric imaging (see Fig. 2). An
245 arrow marks the location on the fibrous cap from which
246 infrared spectra were obtained. Fig. 3 depicts representative
247 spectra from a small area of the fibrous cap. A total of 80,600
248 spectra were obtained from all plaque sections.

2.2. Instrumentation 249

250 The infrared microspectrometer used at beamline U2b of
251 the vacuum ultraviolet (VUV) storage ring of the National
252 Synchrotron Light Source (NSLS) at Brookhaven National
253 Laboratory (BNL), Upton NY consisted of a Nic PLAN[®]

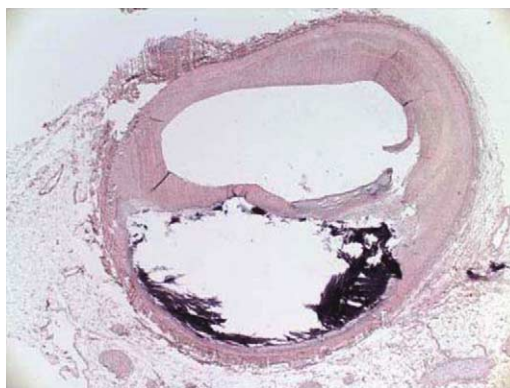


Fig. 1. Stained section of human coronary vulnerable atherosclerotic plaque, obtained as a visible light image. This section was adjacent to the one used for IR microspectrometric imaging.

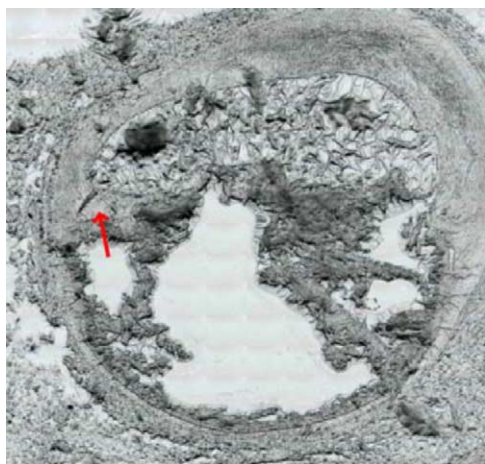


Fig. 2. Unstained section of human coronary vulnerable atherosclerotic plaque, mounted in paraffin. Arrow marks location on fibrous cap from which IR spectra were obtained. This section was adjacent to the section stained and imaged in the visible region. The control image section was at the bottom of the vessel, away from the fibrous cap.

254 infrared microscope interfaced to a Nicolet Magna[®] 860
255 infrared spectrometer (Thermo Electron, Madison WI). A
256 liquid nitrogen cooled 250 cm MCT detector that had
257 maximum signal intensity at 1250 μm was used.

258 Schwartzchild 32 \times and 10 \times all reflecting mirror lenses
259 were used for the objective and condenser, respectively. A
260 remote projected image plane mask before the objective
261 produced the apertures used for single point spectra or raster
262 scan mapping via a digitally controlled motorized micro-
263 scope stage. Spectra were recorded in a reflection absorption
264 mode. A clear location on the infrared reflecting microscope
265

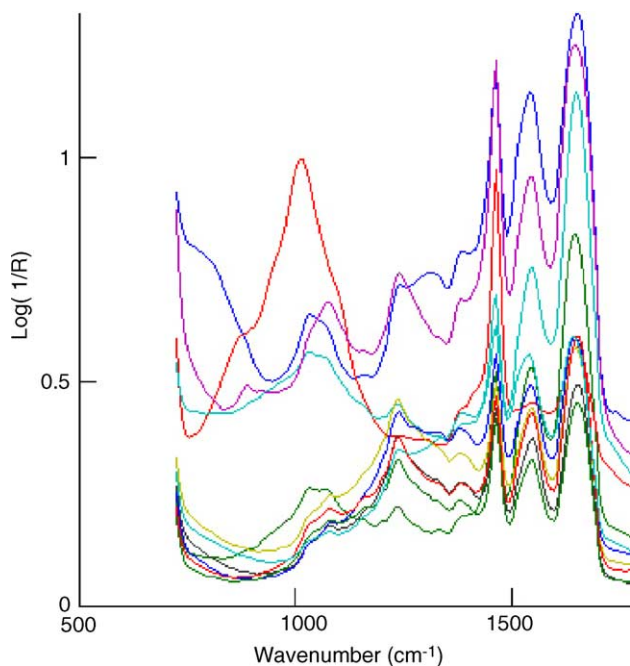


Fig. 3. Representative infrared spectra from the region near the arrow in Fig. 2. The sharp peak at 1469 cm^{-1} arises from paraffin.

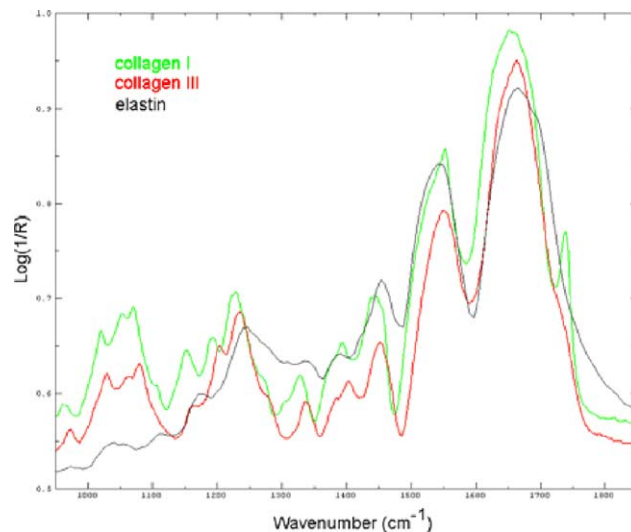


Fig. 4. Spectra of lyophilized standards of collagen I, III, and elastin.

slide ReflectIR[®] (SensIR, Danbury CT) was used to obtain a
265 reflection background spectrum. 266

267 Mapping was also accomplished from a global source
268 focal plane array instrument. The Perkin-Elmer Spotlight
269 model 300 was used to obtain rectangular maps of select
270 regions of the sections being examined. For focal plane array
271 images, the 6.25 $\mu\text{m} \times 6.25 \mu\text{m}$ pixel size was used.

272 Preliminary examination of each map was done from a
273 locally baseline corrected peak area for the triplet at
274 1236 cm^{-1} and the doublet associated with the 1082 cm^{-1}
275 band. A map of the ratio of the area of the 1236 cm^{-1} band to
276 that of the 1082 cm^{-1} was used to locate the region with the
277 highest relative amount of the collagen I.

278 Reference FTIR spectra of collagens I, III, and elastin
279 (Sigma) were obtained (see Fig. 4). While such reference

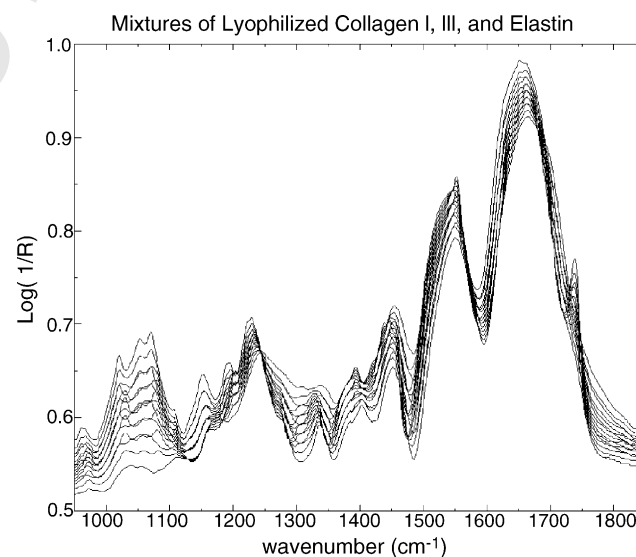


Fig. 5. Spectra of standard mixtures of collagen I, III, and elastin used for mean-centered correlation analysis.

280 compounds are sometimes contaminated by small amounts
 281 of lipid, potential contamination posed no problem for this
 282 research because the lipid regions of the spectrum were not
 283 used in the analysis to avoid the paraffin. The spectral data
 284 were scatter-corrected prior to data analysis (see Fig. 5).
 285 Representative spectra from a human coronary tissue section
 286 are presented in Fig. 3 for comparison with Fig. 5. The sharp
 287 peak at 1469 cm^{-1} in Fig. 3 arises from paraffin. The
 288 chemical composition of the tissue samples between
 289 adjacent areas of tissue is typically similar, and as a result,
 290 the gross appearances of the spectra are similar.

291 SEM morphometry provided the reference method for
 292 collagens and elastin [20]. A contract laboratory (Industrial
 293 Analytical Services, Leominster, MA) was used to blind the
 294 spectroscopists and electron microscopists examining the
 295 tissue sections. A similar methodology was employed by the
 296 authors in a previous near-IR study of aneurysm6.

297 2.3. Data analysis

298 Analytical software was written in Matlab 6.5 (The Math
 299 Works, Inc., Natick, Mass.). In an effort to determine which
 300 spectral changes in the coronary sections were associated
 301 with collagens I and III and elastin composition changes, a
 302 set of sample mixtures of collagens I and III and elastin was
 303 prepared using pure lyophilized standards (see Fig. 5). A
 304 triangular array of compositions was constructed for this
 305 study similar to the one used in Ref. [6]. The composition of
 306 each of the prepared sample standards was represented by a
 307 vertex in the array, with the pure collagen I (C1) standard in
 308 one corner of the triangle, the pure collagen III (C3) in
 309 another corner of the triangle, and finally the pure elastin in
 310 the remaining corner of the triangle. The concentrations of
 311 each constituent in the standard mixtures were set at 0, 25,
 312 50, 75, or 100 wt.% of each lyophilized protein. The
 313 vertexes represent all possible combinations of mixtures in
 314 the percentages given (a total of 15 mixtures including the
 315 pure corner standards). The center (i.e., group mean) would
 316 represent a mixture of one-third of each protein, but this

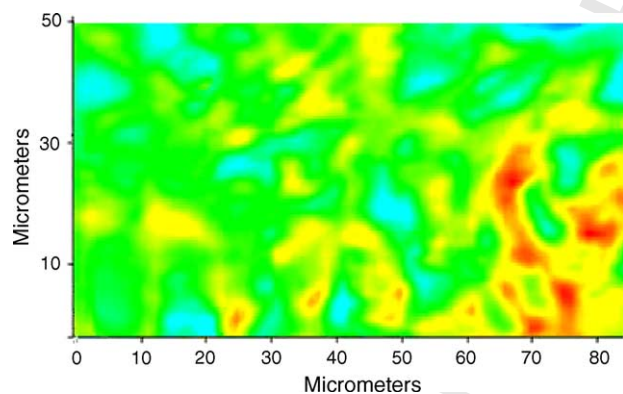


Fig. 6. Collagen I distribution in targeted region of fibrous cap (red = high, blue = low concentration). (For interpretation of the references to color in this figure legend, the reader is referred to the web version of the article.)

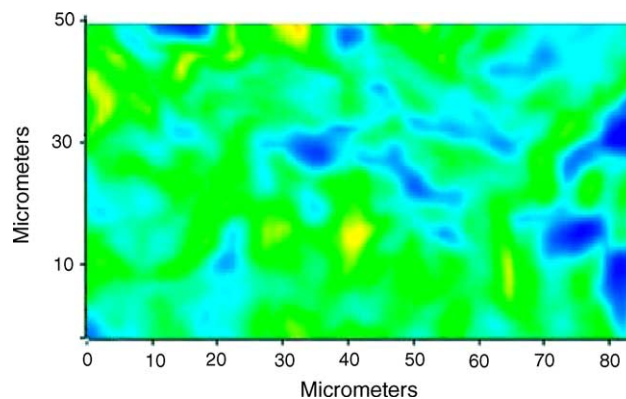


Fig. 7. Collagen III distribution in targeted region of fibrous cap (yellow = high, blue = low concentration). (For interpretation of the references to color in this figure legend, the reader is referred to the web version of the article.)

317 sample was not actually prepared in the set. The reflection
 318 spectra of the 15 mixtures were compared to the reflection
 319 spectra of the coronary sections by mean-centering the
 320 spectra of the mixtures and the spectra of the coronary artery
 321 sections. The difference spectra between each standard
 322 sample spectrum and the mean spectrum of the standard
 323 samples were calculated. Likewise, the difference spectra
 324 between each coronary section spectrum and the mean
 325 spectrum of the coronary sections were also calculated.
 326 Finally, the difference spectra of the standards and the
 327 coronary sections were then correlated using the product-
 328 moment correlation coefficient. The values of these
 329 correlation coefficients were contour plotted to produce
 330 images corresponding to collagen I, III, and elastin in
 331 Figs. 6–9.

3. Results and discussion

332 The correlations between the coronary tissue section
 333 spectra and the set of standard sample spectra ranged
 334 between ± 0.99 . In consequence, the contours in Figs. 6–8
 335 covered a wide range of correlation values (as did the pixels
 336

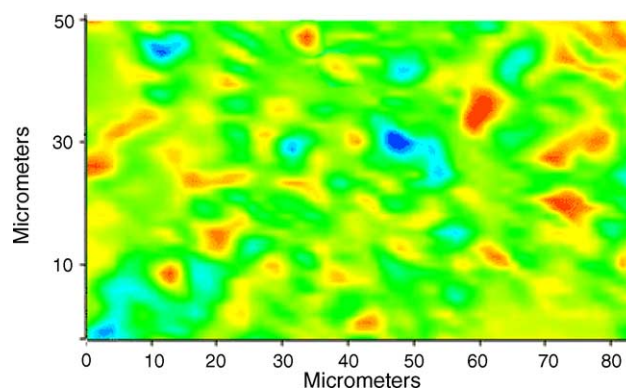


Fig. 8. Elastin distribution in targeted region of fibrous cap (red = high, blue = low concentration). (For interpretation of the references to color in this figure legend, the reader is referred to the web version of the article.)

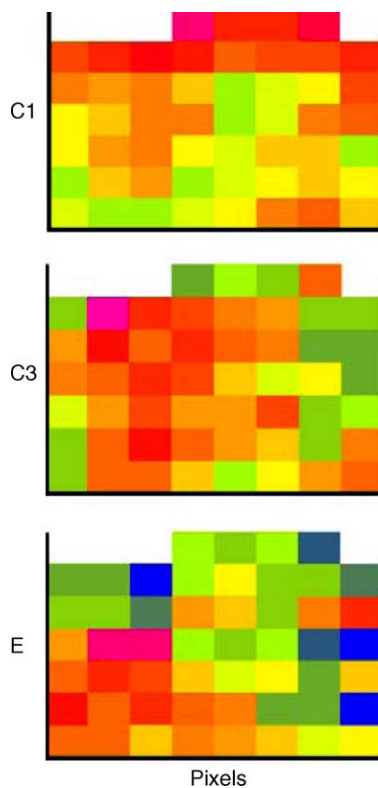


Fig. 9. Localized distribution of collagen I, collagen III, and elastin at individual pixel resolution.

in Fig. 9). Color was used to represent correlation between the spectra of the coronary sections and reference standards. Violet represents the lowest correlation, while red represents the highest. The region at the far left of Figs. 6–8, off the edge of the thin cap, served as a sort of internal standard or control for the images as the scanning progressed toward the right and the thinnest portion of the cap.

Fig. 6 shows the correlation between the tissue spectra and amount of collagen I in the standards in the region marked by the arrow in Fig. 2. Pixel values were interpolated between the concentrations of the standards to reach the maximum correlation, as performed in Ref. [6]. While the amount of collagen I does not increase monotonically from left to right in the image, there is a gradient in concentration over the 80 μm distance across the fibrous cap. The right side of the image in Fig. 6 is the side closest to the thinnest area of the fibrous cap, as shown in Fig. 1.

Fig. 7 depicts the distribution of collagen III predicted in a similar manner. Collagen III also shows an overall gradient, but instead generally decreases nonmonotonically from left to right in the image. In contrast, the amount of elastin did not appear to change substantially across the field of the image (see Fig. 8). However, most of the loss of elastin could have occurred long before the coronary tissue was collected. The control section imaged at the bottom of the vessel was similar to Fig. 8 in that it showed no obvious concentration trends for either the collagens or elastin. Overall, the trends in collagen I, III, and elastin observed in

human coronary plaque are similar to those observed in AAA. At single pixel resolution on the right side of the sample zone nearest the thinnest region of the fibrous cap (see Fig. 9), gradients are not as clear.

Rupture-prone plaques are not the lone vulnerable plaques. All categories of atherosclerotic plaques with high probability of thrombotic complications and swift progression should be regarded as vulnerable plaques. Furthermore, vulnerable plaques are not the only culprit features leading to the occurrence of acute coronary syndromes, myocardial infarction, and sudden cardiac death. Vulnerable blood (i.e., blood inclined toward thrombosis) and vulnerable myocardium (inclined toward lethal arrhythmia) perform an essential role in the clinical outcome. The phrase “vulnerable patient” has even been proposed for the classification of persons with high probability of emergent cardiac events in the near future. A quantitative means of cumulative risk assessment of vulnerable patients should be created that includes variables describing plaque, blood, and myocardial vulnerability. Newly developed assays (e.g., for C-reactive protein), imaging techniques (e.g., CT and MRI), non-invasive electrophysiological tests (for vulnerable myocardium), and promising catheters (to localize and characterize vulnerable plaque), together with prospective genomic and proteomic methods, will lead researchers in the hunt for vulnerable patients. These analytical methods will also lead to the expansion and exploitation of new therapies, and eventually to reduction in the incidence of acute coronary syndromes and sudden cardiac death.

This preliminary study has some important limitations. A single patient served as the source of the 80,600 spectra collected from 24 coronary sections, limiting the observable variation in the data set. The lack of detailed histological data for the samples and lack of clinical history from the patient prevents the association of the spectra with specific tissue pathologies and comparison of pathology. Most importantly, the exact location of any rupture (the culprit lesion) was not uncovered in the tissue sections. For this reason, the exact nature of the gradients within 10 μm of any tear in the fibrous cap cannot be determined. However, the fact that gradients in collagen and elastin similar to those observed in AAAs do exist in the vicinity of a plaque rupture suggests that similar mechanisms of protein degradation may be responsible in both disease states. Thus, an increase in collagen I at the expense of collagen III (and possibly of elastin) might serve as a marker of plaques needing an immediate intervention.

4. Conclusion

Like near-IR spectra, mid-IR spectra are distinctive for proteins in the blood vessel wall (specifically collagens and elastin). The results of this preliminary study suggest that synchrotron IR microspectroscopy is a potentially useful technique for investigating vascular changes and protein

418 composition associated with cardiovascular disease. In
 419 particular, synchrotron IR microspectroscopy has the light
 420 intensity, and thus spatial resolution using small mask
 421 apertures, needed to quantify collagens and elastin within
 422 10 μm of the site of plaque rupture. These early results
 423 support an expanded study in the future employing IR
 424 spectra to characterize completely chemical compositions
 425 within 10 μm of the location of plaque rupture. If the
 426 compositions of many of these small regions prove similar in
 427 many different patients, a useful marker will have been
 428 demonstrated that can be targeted by near-IR catheters in
 429 vivo.

430 Acknowledgment

431 This work was supported in part by KSEF-148-502-03-61
 432 and by the Kansas State University Microbeam Spectro-
 433 scopy Laboratory. The research was carried out in part at the
 434 National Synchrotron Light Source, Brookhaven National
 435 Laboratory, which is supported by the U.S. Department of
 436 Energy, Division of Materials Sciences and Division of
 437 Chemical Sciences, under Contract No. DE-AC02-
 438 98CH10886. The work could not have been performed
 439 without the invaluable technical assistance of Tiffany Fisher
 440 (KSU), Nebojsa Marinkovic (NSLS), and Randy Smith
 441 (NSLS).

442 References

- 443 [1] M. Naghavi, P. Libby, E. Falk, S.W. Casscells, S. Litovsky, R.A.
 444 Lodder, P.K. Shah, J.T. Willerson, From vulnerable plaque to vulner-
 445 able patient: a call for new definitions, *Circulation* 108 (14) (2003)
 446 1664–1672.
- 447 [2] F.D. Kolodgie, A.P. Burke, A. Farb, et al. The thin-cap fibroatheroma:
 448 a type of vulnerable plaque: the major precursor lesion to acute
 449 coronary syndromes, *Curr. Opin. Cardiol.* 16 (2001) 285–292.
- 450 [3] R.W. Wissler, J.P. Strong, Risk factors and progression of athero-
 451 sclerosis in youth. PDAY Research Group. Pathological determinants
 452 of atherosclerosis in youth, *Am. J. Pathol.* 153 (1998) 1023–1033.
- 453 [4] E.M. Tuzcu, S.R. Kapadia, E. Tutar, et al. High prevalence of coronary
 454 atherosclerosis in asymptomatic teenagers and young adults: evidence
 455 from intravascular ultrasound, *Circulation* 103 (2001) 2705–2710.
- 456 [5] G. Pasterkamp, A.H. Schoneveld, A.C. van der Wal, et al. Relation of
 457 arterial geometry to luminal narrowing and histologic markers for

- plaque vulnerability: the remodeling paradox, *J. Am. Coll. Cardiol.* 32
 (1998) 655–662. 458
- [6] A. Urbas, M.W. Manning, A. Daugherty, L.A. Cassis, R.A. Lodder,
 Near-infrared spectrometry of abdominal aortic aneurysm in the ApoE
 –/– mouse, *Anal. Chem.* 75 (14) (2003) 3650–3655. 459
 460
 461
 462
- [7] P.R. Moreno, R.A. Lodder, K.R. Purushothaman, W.E. Charash, W.N.
 O'Connor, J.E. Muller, Detection of lipid pool, thin fibrous cap, and
 inflammatory cells in human aortic atherosclerotic plaques by near-
 infrared spectroscopy, *Circulation* 105 (8) (2002) 923–927. 463
 464
 465
 466
- [8] L.A. Cassis, R.A. Lodder, *Anal. Chem.* 65 (9) (1993) 1247–1256. 467
- [9] R.J. Dempsey, R.A. Lodder, *Ann. N. Y. Acad. Sci.* 820 (1997) 149–
 169. 468
 469
- [10] L.A. Cassis, W.C. Symons, R.A. Lodder, Cardiovascular near-infrared
 imaging, *J. Near-Infrared Spectrom.* 6 (1998) A21–A25. 470
 471
- [11] L.A. Cassis, A. Urbas, R.A. Lodder, Hyperspectral integrated com-
 putational imaging, *Anal. Bioanal. Chem.* (2004)10.1007/s00216-
 004-1. 472
 473
 474
- [12] J.M. Gentner, E. Wentrup-Byrne, P.J. Walker, M.D. Walsh, Compar-
 ison of fresh and post-mortem human arterial tissue: an analysis using
 FT-IR microspectroscopy and chemometrics, *Cell Mol. Biol. (Noisy-
 le-grand)* 44 (1) (1998) 251–259. 475
 476
 477
 478
- [13] R. Manoharan, J.J. Baraga, R.P. Rava, R.R. Dasari, M. Fitzmaurice,
 M.S. Feld, Biochemical analysis and mapping of atherosclerotic
 human artery using FT-IR microspectroscopy, *Atherosclerosis* 103
 (2) (1993) 181–193. 479
 480
 481
 482
- [14] A. Becker, M. Epple, K.M. uller, I. Schmitz, A comparative study of
 clinically well-characterized human atherosclerotic plaques with his-
 tological, chemical, and ultrastructural methods, *J. Inorg. Biochem.* 98
 (12) (2004) 2032–2038. 483
 484
 485
 486
- [15] E. Wang, K. Thyagarajan, R. Tu, D. Lin, C. Hata, S.H. Shen, R.C.
 Quijano, Evaluation of collagen modification and surface properties of
 a bovine artery via polyepoxy compound fixation, *Int. J. Artif. Organs*
 16 (7) (1993) 530–536. 487
 488
 489
 490
- [16] A. Singla, C.H. Lee, Effect of elastin on the calcification rate of
 collagen-elastin matrix systems, *J. Biomed. Mater. Res.* 60 (3) (2002)
 368–374. 491
 492
 493
- [17] L. Silveira Jr., S. Sathaiiah, R.A. Zangaro, M.T. Pacheco, M.C.
 Chavantes, C.A. Pasqualucci, Near-infrared Raman spectroscopy of
 human coronary arteries: histopathological classification based on
 Mahalanobis distance, *J. Clin. Laser Med. Surg.* 21 (4) (2003)
 203–208. 494
 495
 496
 497
 498
- [18] A. Daugherty, M.W. Manning, L.A. Cassis, Angiotensin II promotes
 atherosclerotic lesions and aneurysms in apolipoprotein E-deficient
 mice, *J. Clin. Invest.* 105 (2000) 1605–1612. 499
 500
 501
- [19] V. Neumeister, M. Scheibe, P. Lattke, W. Jaross, Determination of the
 cholesterol-collagen ratio of arterial atherosclerotic plaques using near
 infrared spectroscopy as a possible measure of plaque stability,
Atherosclerosis 165 (2) (2002) 251–257. 502
 503
 504
 505
- [20] A.M. Sharifi, J.S. Li, D. Endemeann, E.L. Schiffrin, Effects of
 enalapril and amlodipine on small-artery structure and composition,
 and on endothelial dysfunction in spontaneously hypertensive rats, *J.*
Hypertension 4 (1998) 457–466. 506
 507
 508
 509

510

UNCORRECTED